scientific reports

Check for updates

OPEN

Improving human cardiac organoid design using transcriptomics

Nathaniel A. Hyams[1], Charles M. Kerr[2], Dimitrios C. Arhontoulis[2], Jean Marie Ruddy[3] & Ying Mei[1,4]✉

Cardiovascular disease (CVD) is the leading cause of death worldwide. To this end, human cardiac organoids (hCOs) have been developed for improved organotypic CVD modeling over conventional in vivo animal models. Utilizing human cells, hCOs hold great promise to bridge key gaps in CVD research pertaining to human-specific conditions. hCOs are multicellular 3D models which resemble heart structure and function. Varying hCOs fabrication techniques leads to functional and phenotypic differences. To investigate heterogeneity across hCO platforms, we performed a transcriptomic analysis utilizing bulk RNA-sequencing from four previously published unique hCO studies. We further compared selected hCOs to 2D and 3D hiPSC-derived cardiomyocytes (hiPSC-CMs), as well as fetal and adult human myocardium bulk RNA-sequencing samples. Upon investigation utilizing Principal Component Analysis, K-means clustering analysis of key genes, and further downstream analyses such as Gene Set Enrichment (GSEA), Gene Set Variation (GSVA), and GO term enrichment, we found that hCO fabrication method influences maturity and cellular heterogeneity across models. Thus, we propose that adjustment of fabrication method will result in an hCO with a defined maturity and transcriptomic profile to facilitate its specified applications, in turn maximizing its modeling potential.

Keywords Human cardiac organoids, Modeling, Bulk RNA-sequencing

Cardiovascular disease (CVD) is the leading cause of death worldwide[1–3]. Additionally, cardiotoxicity is commonly implicated in novel drug development failure[4]. To address these challenges, significant efforts have been devoted to developing in vitro systems for the modeling of adult human hearts[5–9]. Animal models have limitations that hinder their ability to faithfully replicate CVD[10]. Small animal models like mice and rats lack important biological features of human hearts, such as a high heart rate, which prevents the accurate modeling of conditions like arrhythmia. On the other hand, large animal models such as pigs and monkeys are more biologically similar to humans but are difficult to maintain within research contexts. Recent progress in cardiac differentiation of human induced pluripotent stem cells (hiPSCs) has allowed for functional, reproducible, and highly enriched populations of human cardiac cells for disease modeling[11–14]. hiPSC-cardiomyocytes (hiPSC-CMs) cultured on 2D substrates have been used extensively to model both various forms of CVD as well as drug-induced cardiotoxicity[15–17]. Despite progress, 2D hiPSC-CMs inadequately capture intricate cell–cell and cell–matrix interactions which occur in 3D within the body[18,19]. 3D cell culture has allowed for improved replication of in vivo architectures, bolstering modeling capabilities[20,21]. Specifically, 3D hiPSC-CM culture systems offer a higher level of cardiac lineage specification, and an upregulation in troponin expression[22]. To this end, 3D human cardiac organoids (hCOs) have been developed to close the gap between 2D in vitro culture and the cardiac tissue subject to being modeled[23–26]. While there is discourse over defining features, hCOs generally share a set of basic characteristics: (1) multiple cell types to mimic native myocardial cellular composition, (2) structural complexity resembling a tissue-level function, and (3) the ability to mature as culture duration increases. hCOs have enabled superior biomimicry of native cardiac tissue structure and function, more accurately recapitulating both cardiac development and various cardiac pathologies[27–32].

To date, there are three primary strategies for hCO fabrication: (1) hCOs which form through directed cardiac differentiation of 3D embryoid bodies (EBs), (2) engineered hCOs which utilize matured/differentiated cells and take advantage of 3D self-assembly mechanics, and (3) a hybrid between the two[23,29,31]. This variety in approach results in heterogeneity between hCOs, providing a unique opportunity to tailor models towards a specific developmental mechanism or to target a disease of interest. Here, we leverage existing RNA sequencing

[1]Bioengineering Department, Clemson University, Clemson, SC 29631, USA. [2]Molecular and Cellular Biology and Pathobiology Program, Medical University of South Carolina, Charleston, SC 29425, USA. [3]Division of Vascular Surgery, Department of Surgery, Medical University of South Carolina, Charleston, SC 29425, USA. [4]Department of Regenerative Medicine and Cell Biology, Medical University of South Carolina, Charleston, SC 29425, USA. ✉email: mei@clemson.edu

(RNA-seq) datasets from across four unique hCO studies to examine the effects of the aforementioned diversity of fabrication methods[27,29,30,33]. We include both 2D and 3D hiPSC-CMs to account for 3D environment and multicellularity effects on the transcriptome[34,35]. In addition, to compare each model's similarity to human myocardium at both developing and mature stages, we include fetal and adult myocardial samples[30,36]. This will enhance our understanding as to how hCOs relate to standard 2D in vitro modeling and to cardiac tissue itself. In this study, we aim to encapsulate the diversity of the hCO field within the unique datasets sampled with the goal of gaining transcriptomic insight into hCO application, and how to optimize hCO design for its intended use. Our results showed that transcriptomic proximity to native myocardium is proportional to model maturity, while also highlighting unique transcriptomic profiles between hCOs. Furthermore, we conclude that specific hCO application should drive fabrication methods in order to maximize potential.

Results

Select representative hCO models

We compiled bulk RNA-seq datasets from four unique hCOs to provide a wholistic overview of the current hCO field[27,29,30,33]. These four studies were selected as they embody a range of fabrication methods, from 3D EB-based cardiac differentiation to engineered microtissue assembly. Lewis-Israeli et al. developed the herein termed EB hCO, which utilized 3D EBs as a base platform, then induced cardiac mesoderm via Wnt pathway activation/inhibition, supplemented with a second Wnt pathway activation step (Fig. S1A)[27]. As a result, EB hCOs profiled similarly to the developing fetal heart, with biomimetic cell lineage ratios and a robust cardiogenic progression. Ergir et al. extended a widely accepted 2D hiPSC cardiac differentiation protocol by resuspending cells after 2D differentiation into 3D microwells for hCO formation (Fig. S1B)[29]. The result was a promotion in cardiomyocyte (CM) survival during an extended culture period. Denoted as Primary Stroma hCO, Richards et al. took advantage of self-organizing principles to form their hCO model in agarose microwells (Fig. S1C)[31]. hiPSC-CMs acquired commercially along with a mixed population of human primary stromal cells provided robust maturity and a defined cellular makeup, which resulted in a reproducible modular system. The HeartDyno hCO, developed by Mills et al. used an in-house 2D cardiac differentiation protocol to induce a 70% hiPSC-CM to 30% CD90 + stromal cell ratio, followed by the seeding of differentiated cells into an engineered system in order to measure functional readouts such as contraction force (Fig. S1D)[30]. This increased hCO throughput for the testing and development of novel cardioactive drugs, as the scalability and ease of modulation in this system make it possible to determine numerous key drivers of CM maturation within their model. hCO samples were selected carefully, as all possessed bulk RNA-seq data while simultaneously representing a comprehensive range of hCO approaches. In addition, we included 2D and 3D hiPSC-CM samples in addition to human fetal and adult myocardial bulk RNA-seq data in our analysis to allow for hCOs to be compared to both the standard 2D in vitro model as well as the myocardium (Figure S2A)[35,37]. This established a range of perceived maturity in order to assess how hCOs fit. This provided a scaled platform with which to identify genes of interest that were significantly changed for further analysis of transcriptomic divergence which could be explored via Principal Component Analysis, Gene Set Enrichment Analysis, K-Means clustering analysis, and GO term enrichment analysis (Fig. 2B&C)[38].

hCOs improve modeling potential, boosting transcriptomic proximity to human cardiac tissue

Principal component analysis (PCA) was performed to identify transcriptomic influences toward variation across the hCO systems investigated, 2D and 3D hiPSC-CMs, and in vivo fetal and adult myocardium data (Fig. 1A). The PC1 and PC2 axes of the PCA plot, accounting for 36.9% and 28.2% of total variation between samples, respectively, reveal distinct separation of hCO samples from CM-only samples, replicating previously reported trends[34]. Based on the relative positions of 2D and 3D hiPSC-CMs in addition to human fetal and adult myocardial samples, we reasoned PC1 to be an index for maturation. Fetal myocardial samples cluster lower on PC1 than their adult counterparts, indicative that maturity increases alongside PC1. Supporting this, hiPSC-CM samples, known to be immature, group lower than both hCO and in vivo samples, supporting our hypothesized PC index[39,40]. hCO samples grouping between hiPSC-CM samples and in vivo tissue across PC1 supports findings which implicate 3D hCO models promoting cellular maturity and the subsequent ability to form organotypic structures.

PC2 was interpreted as a measure of cellular heterogeneity for samples. At the bottom of PC2 were homogeneous populations of 2D and 3D hiPSC-CMs. Meanwhile, Embryoid Body (EB) hCOs, which reported a high number of endo-, myo- and epicardial lineages, represent the most varied samples. Supporting this, we identified Primary Stroma hCOs, which possess four defined cell types, to be lower than Extended Culture and HeartDyno hCOs. Extended Culture and HeartDyno hCOs report more diverse cell populations than Primary Stroma hCO, as both models used less defined cell populations. This reiterates PC2 to be a measure of cellular heterogeneity within a sample.

GSEA establishes maturity and heterogeneity as key factors in hCO diversity

To reveal key biological processes underpinning PC1 and PC2 as indices for maturation and cellular heterogeneity, respectively, we conducted Gene Set Enrichment Analysis (GSEA) across both PC1 and PC2. GSEA was utilized to determine significantly enriched biological pathways within sample groups[41]. Only significant (FDR < 0.25) and relevant pathways were included in our analysis. To provide a concise depiction of GSEA trends, the normalized enrichment score (NES) of key significant pathways were displayed in Fig. 1B&C. This provides an unbiased approach to uncover biological pathways which drive sample placement within our PCA at the extreme ends of PC1 and PC2.

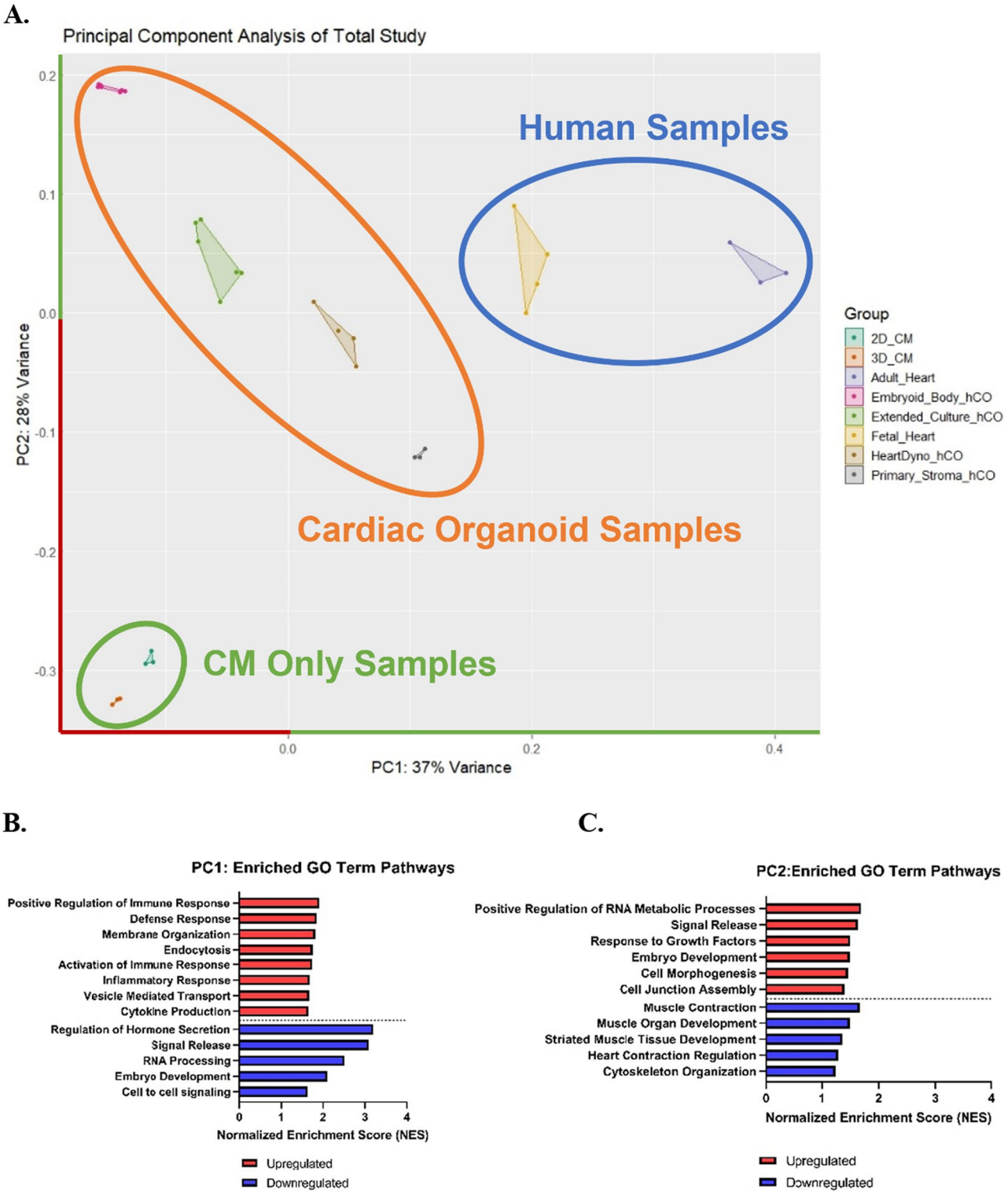

Figure 1. PCA encompassing the whole study, along with GSEA interpretation of each axis. (**A**) Principal component analysis (PCA) detailing representative hCO models: Embryoid Body hCO (n = 9), Extended Culture hCO (n = 6), HeartDyno hCO (n = 4), and Primary Stroma hCO (n = 3). These were included in relation to both adult (n = 3) and fetal (n = 4) human myocardial RNA-seq samples as well as cardiomyocyte samples in both 2D (n = 3) and 3D (n = 3). (**B**) Gene set enrichment analysis (GSEA) across the PC1 axis, displaying significant, selected GO terms pathways of interest. Across PC1, immune-centric pathways were positively enriched, while pathways indicating cell–cell crosstalk were negative enriched. (**C**) Gene set enrichment analysis (GSEA) across the PC2 axis. Selected, significant pathways indicated that cell morphogenic pathways were positively enriched, while cardiac-specific pathways were negatively enriched.

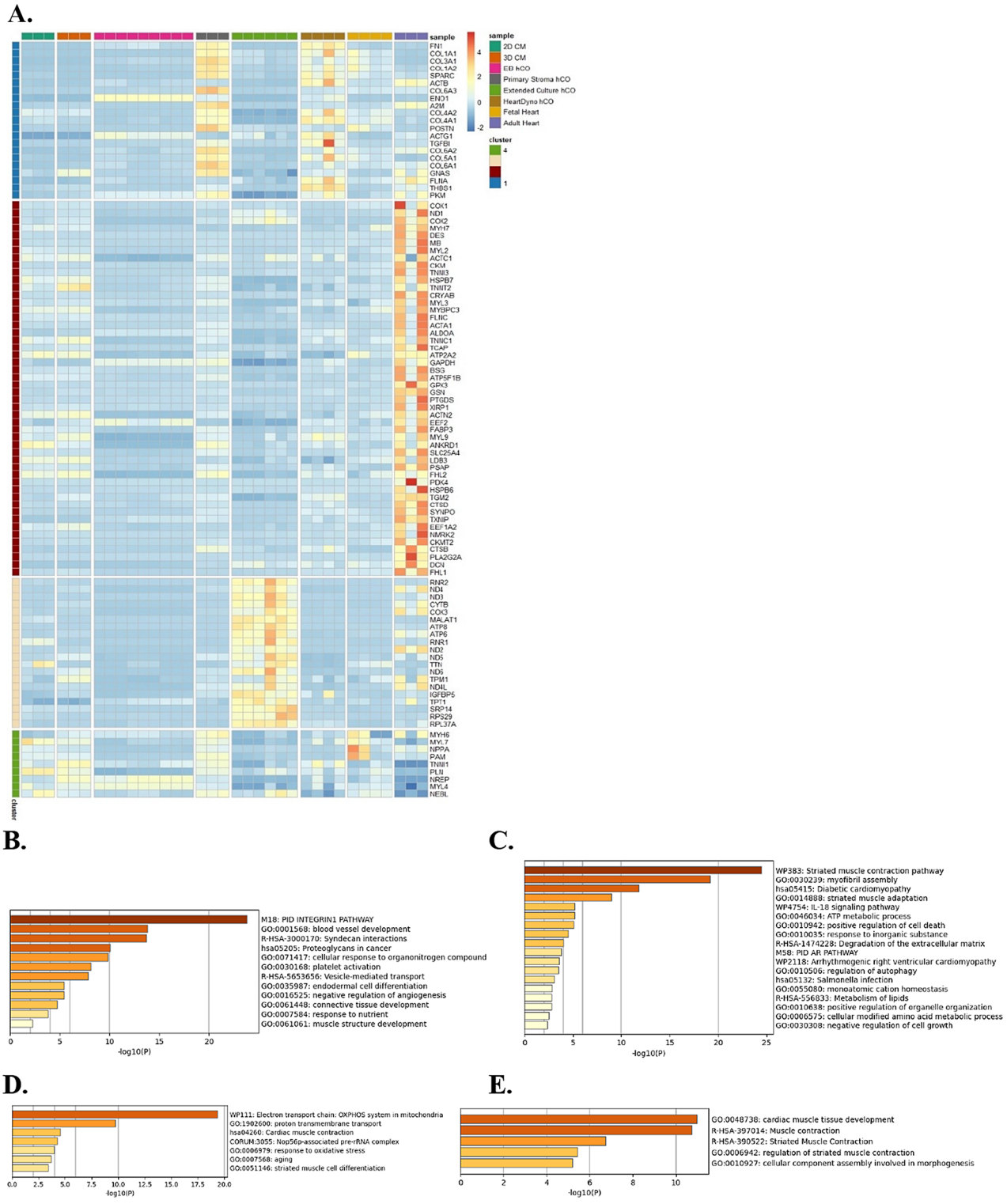

Figure 2. (**A**) K-means clustering heatmap of the top 100 genes driving variability across all samples reveals distinct expression profiles between different hCO samples and human myocardial samples. Vertical groups represent sample sets, while horizontal groups represent the four cluster groups which K-means analysis divided these 100 genes. Scale is Z-score. (**B**) Metascape pathway analysis of Cluster 1 indicates strong ECM capability, structure, and function within samples with high relative expression. (**C**) Metascape pathway analysis of Cluster 2 indicates presence of a matured myocardium within samples with high relative expression. (**D**) Metascape pathway analysis of Cluster 3 indicates presence of a matured metabolic response, particularly in the production of ATP and oxidative phosphorylation within samples with high relative expression. (**E**) Metascape pathway analysis of Cluster 4 indicates an enrichment towards cardiac developmental pathways.

GSEA showed that PC1 is positively enriched in gene ontology (GO) pathways associated with inflammatory response, cytokine production, and membrane organization (Fig. 1B). Due to in vivo samples grouping at the upper extreme of PC1, we speculated that the presence of resident immune cell populations found within in vivo cardiac tissues is responsible for immune-centric GO pathway enrichment. Conversely, GSEA indicated negative enrichment across PC1 in GO pathways associated with development and cell plasticity, including embryo development and signal release (Fig. 1B). hip SC-CM and EB hCO samples clustered as the bottom of PC1, pointing towards an immature profile in relation to other hCO and myocardial samples. GO pathways enriched across PC1 via GSEA contextualize and support our prior assertion that PC1 represents maturity across samples.

Across PC2, GSEA supported our proposed index of cellular heterogeneity, as pathways such as cell morphogenesis, embryo development, and cell junction assembly were significantly positively enriched (Fig. 1C). Highlighted pathways implicated samples on the extreme upper end of PC2 possessed developmental, and thus diverse, cell lineages. Heterogeneous samples such as EB hCOs grouped on the upper end of PC2, reinforcing the variable nature of 3D differentiation methods[42]. Conversely, muscle contraction and striated muscle tissue development pathways were enriched along the negative end of PC2, influenced by homogeneous hiPSC-CM samples. GSEA provided biological context for PCA sample placement and confirmed our PC axis assumptions of maturity and heterogeneity, clarifying the understanding of how hCOs improve modeling capabilities.

k-means analysis infers specific hCO strengths and potential niches

GSEA, while informative of general trends, does not identify specific genes associated with key cardiac biological functions. To address this, we sought to holistically investigate expression of genes within our dataset which could reveal further differences between hCOs. To achieve this, we implemented K-means clustering, an unsupervised machine learning algorithm which clusters data points based on similarity[43]. In our study, we pursued the 100 most variable genes between samples and applied K-means clustering to this gene set. Upon analysis, the data separated into four distinct clusters, illustrating strengths of analyzed hCO models (Fig. 2A). Additionally, we generated a heatmap, highlighting biological processes of interest across samples (Fig. S3). This provided us with a targeted view of key cardiac process expression profiles for each sample set.

Cluster 1 (Fig. 2A) consisted of 21 genes and was associated with Primary Stroma and HeartDyno hCOs showcasing a high expression of extracellular matrix (ECM) encoding genes, including COL1A1, COL4A1, and FN1. These genes play an integral role in ECM formation, particularly in collagen and fibronectin synthesis, and are vital to cell adhesion, migration, and maturation[44]. The cardiac fibroblast population is vital for ECM secretion in the cardiac microenvironment, particularly in pathological conditions; thus, we propose hCOs expressing a robust ECM transcriptomic profile are suitable for modeling disease and drug-induced cardiotoxicity affecting the cardiac stroma[45]. To support the claim of an ECM-enriched profile of Cluster 1 genes, we used Metascape, an online tool which uses a gene list input to generate relevant biological pathways[46]. We prepared the 21 genes contained in Cluster 1 as a gene set for use in this enrichment analysis. We found that cell–cell interaction, angiogenic, and connective tissue developmental pathways were enriched within the Cluster 1 gene set, bolstering HeartDyno and Primary Stroma hCOs as improved ECM-centric disease models within the heart (Fig. 2B).

Cluster 2 (Fig. 2A) highlighted 50 genes highly expressed in in vivo adult myocardial samples. Genes encoding for myosin heavy chain 7 (MYH7), myosin light chain 2 (MYL2), and cardiac troponin 3 (TNNI3) were identified in this cluster, all indicative of a matured myocardial transcriptomic profile[16]. We confirmed this via enrichment analysis in Metascape, as the Cluster 2 gene set suggests myofibril assembly as well as contraction and adaptation of striated muscle are key biological processes, emphasizing a mature, dynamic cardiac profile (Fig. 2C). This finding substantiates a consensus shortcoming within the hCO field, which is the lack of maturity of hiPSC-CMs in hCOs[47].

Cluster 3 (Fig. 2A) accentuated an upregulated transcriptomic profile unique to Extended Culture hCO samples, which we reasoned to be indicative of metabolic maturation. COX3 encodes for a subunit within the cytochrome-c oxidase subunit, which plays an integral role in the termination of oxidative phosphorylation[48]. Likewise, ND4 and ATP6 encode for electron transport chain (ETC) components and functions, including adenosine triphosphate (ATP) synthase machinery or promotion of intermediate energy substrate activity such as NADH[49]. These are all hallmarks of a robust transition from fetal glycolytic to adult oxidative means of energy production in the heart[50]. This is further exemplified within enrichment analysis, as metabolic pathways such as ETC, ion transport across membranes, and response to oxidative stress are all implicated within Cluster 3 (Fig. 2D). It can be reasoned that Extended Culture hCO samples possess an enhanced metabolic activity level in relation to other hCO models. Thus, Extended Culture hCOs may be a suitable model for assessing metabolic mechanisms of CVD.

Cluster 4 (Fig. 2A) paralleled between Primary Stroma hCO and fetal atrial samples. Both groups have a moderately upregulated expression within this cluster, which is implicated in both cardiac muscle development and muscle contraction in enrichment analysis (Fig. 2E). While mild, myosin heavy chain-α (MYH6) and atrial light chain-2 (MYL7) upregulation is of particular interest, as these are present in the fetal heart and precursors to Myosin-α isoforms within mature atria[16,51,52]. This provides the basis for Primary Stroma hCOs as an enhanced model for fetal or atrial specific conditions, related to myosin isoform fate. Ultimately, K-means supplemented with enrichment analysis via Metascape identified underlying pathway-based strengths for hCO models.

Gene set variation analysis emphasizes hCO specification while pointing out shortcomings

To gain further insight into the cellular composition of each hCO model, we used gene set variation analysis (GSVA) to investigate the differing expression levels of key genes within specific cell types of interest[53]. GSVA scores represent the presence of a cell type based upon their transcriptomic hallmarks, such as TNNI3, MYL2,

and ACTN2 for ventricular CMs, for example. To this end, we utilized the Human Heart Cell Atlas to construct gene sets consisting of the top 50 genes expressed in cardiac specific cell types (Supp. Table 1)[54].

Stromal populations investigated via GSVA pointed toward hCOs mirroring strengths displayed within GSEA and K-means analysis. Cardiac fibroblast GSVA scores of Primary Stroma and HeartDyno hCO samples were similar to that of in vivo myocardium samples, inferring robust cardiac fibroblast presence and activity (Fig. 3A). Endothelial cell presence was comparable across hCO groups yet was notably lower than in vivo samples (Fig. 3B). This finding prompts a universal shortcoming in current hCO CVD modeling: the lack of a robust, perfusable vascular network. Notably, advances in endothelial cell incorporation and formation of vascular networks have the promise to bolster hCO development in maximizing model size and complexity[55,56]. Interestingly, in both atrial and ventricular CM populations, Primary Stroma hCOs were comparable to both 2D and 3D CM samples in addition to all in vivo myocardial samples (Fig. 3C&D). We have attributed this to the use of hiPSC-CMs after prolonged culture, rather than the utilization of a freshly differentiated hiPSC-CM population. Lastly, immune cell marker GSVA scores for all four hCO models sat directly in between CM-only and in vivo samples (Fig. 3E). While no current hCO incorporates dedicated immune cells to the best of our knowledge, GSVA indicates that immune marker expression is increased from CM-only models. This could be the result of immunoregulatory effects of which some stromal cells within hCOs, such as endothelial cells and fibroblasts[57]. GSVA aided in our understanding of hCO composition, underscoring the need for further advancement in both vascularization and immune cell incorporation to better understand and model CVD. While GSVA provides only a picture of highly expressed genes and is not fully comprehensive, a window into the composition of each hCO was explored, providing information key to the understanding of how to improve models further.

Investigation of hCO-only data bolsters previous findings

To further investigate heterogeneity between hCO models, we conducted a directed PCA including hCO samples only (Fig. 4A). PC1, accounting for 48% of variance between samples, grouped HeartDyno, Extended Culture, and Primary Stroma hCOs tightly, while EB hCOs separated out to the left. PC2 accounted for 41% of sample variance, showing EB hCO samples grouping in between HeartDyno and Primary Stroma hCOs at the top, while Extended Culture hCOs clustered at the bottom. The manner in which hCOs separated from one another in this PCA shows similar trends to the original PCA conducted. Primary Stroma and HeartDyno hCOs grouped

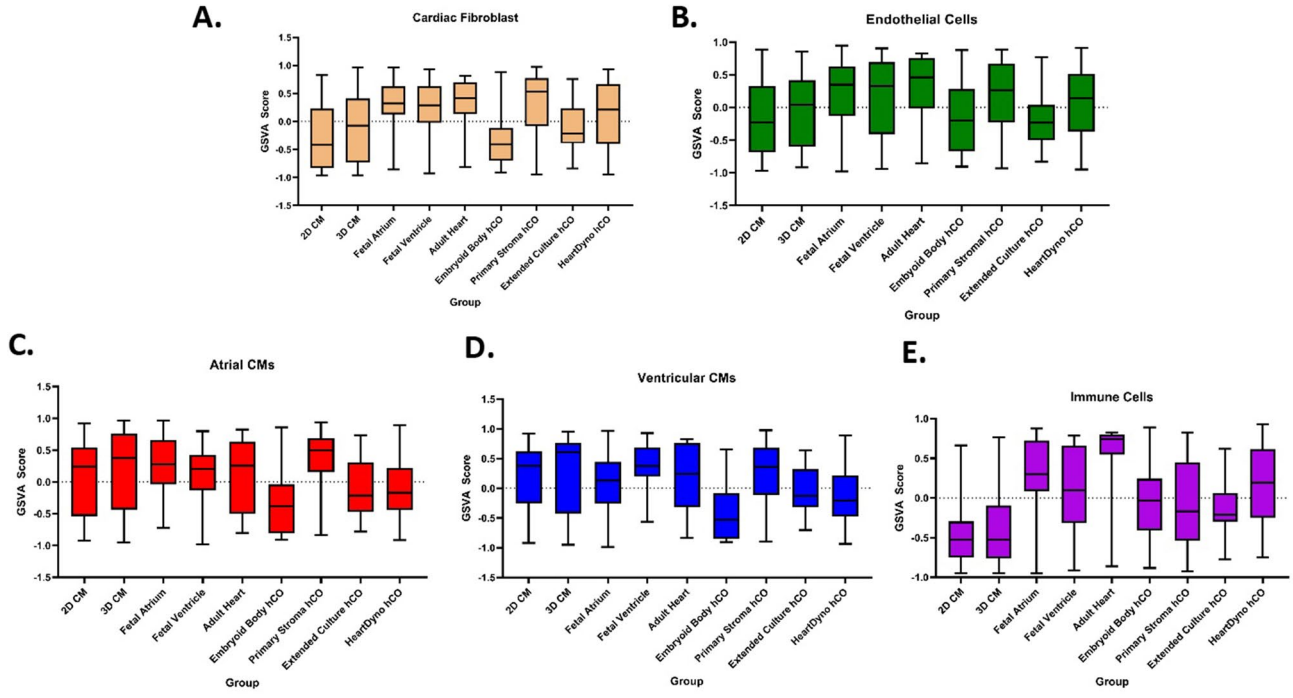

Figure 3. (**A**) Gene Set Variation Analysis (GSVA) of the top 50 expressed Cardiac Fibroblast genes according to the Human Heart Atlas. Primary Stroma and HeartDyno hCOs mirrored adult myocardial samples well, indicating robust cardiac fibroblast activity. (**B**) Gene Set Variation Analysis (GSVA) of the top 50 expressed endothelial cell genes according to the Human Heart Atlas. Primary Stroma and HeartDyno hCOs scored the highest out of any hCO sample set. (**C**) Gene Set Variation Analysis (GSVA) of the top 50 expressed Atrial Cardiomyocyte genes according to the Human Heart Atlas. Primary Stroma hCOs and 3D CMs, along with fetal atrial samples score the highest. (**D**) Gene Set Variation Analysis (GSVA) of the top 50 expressed Ventricular Cardiomyocyte genes according to the Human Heart Atlas. 3D CMs, adult heart samples, and Primary Stroma hCOs score the highest, indicating an abundance of ventricular-type CMs. (**E**) Gene Set Variation Analysis (GSVA) of the top 50 expressed Immune Cell genes according to the Human Heart Atlas. In vivo samples score higher than in vitro samples, highlighting the lack of incorporated immune cells within in vitro CVD modeling.

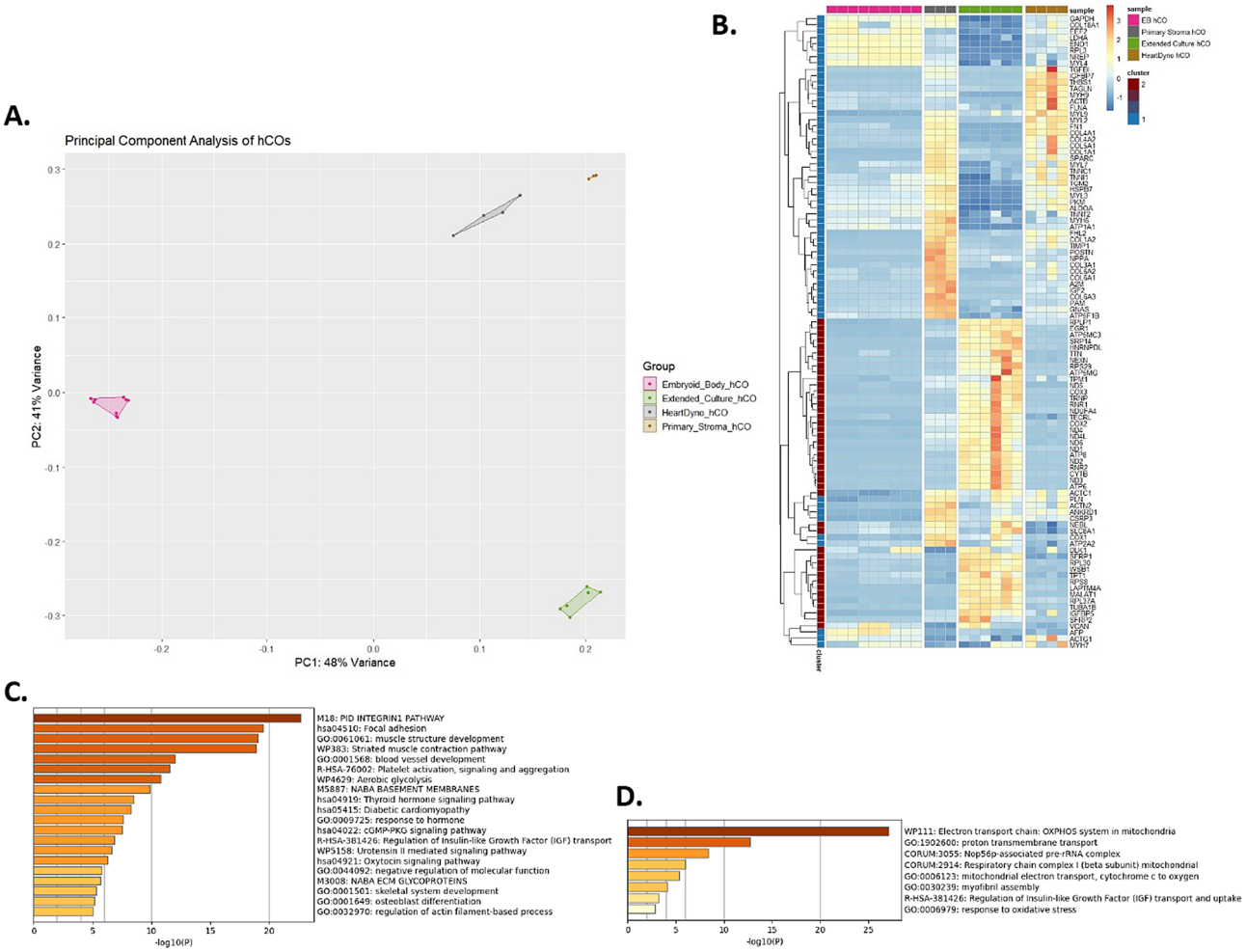

Figure 4. (**A**) Principal component analysis (PCA) detailing representative hCO models investigated (Embryoid Body hCO (n = 9), Extended Culture hCO (n = 6), HeartDyno hCO (n = 4), and Primary Stroma hCO (n = 3)). (**B**) K-means clustering (n = 2 clusters) heatmap of the top 100 genes driving variability across all samples reveals distinct expression profiles between hCO samples. (**C**) Metascape enrichment analysis of Cluster 1 indicates strong ECM capability, structure, and function within samples with high relative expression. (**D**) Metascape enrichment analysis of Cluster 2 indicates presence of a matured myocardium within samples with high relative expression.

together on both PC1 and PC2, meanwhile EB hCOs and Extended Culture hCOs are distinct along PC1 and PC2, respectively.

K-means analysis was then repeated to attain a higher resolution of discrepancy between hCOs (Fig. 4B). In this study, the 100 most variable genes were used, separating into two clusters. Cluster 1 (Fig. 4B) indicated high relative expression in both HeartDyno and Primary Stroma hCOs, including increased expression in genes such as CM markers MYL2 and MYL9 as well as basement membrane component COL4A1. Enrichment analysis via Metascape reiterates our previous findings, as cellular communication, ECM hallmarks, and muscle tissue development are all enriched within Cluster 1 (Fig. 4C). This finding supports the inclusion of a dedicated cardiac fibroblast population if the goal is to model CVD within the cardiac stroma. Cluster 2, consisting of 43 genes, indicated increased metabolic activity within Extended Culture hCOs, as expression of markers such as COX3, ND4, and ATP8 all increased in these samples (Fig. 4B). Enrichment analysis reinforces this, as enriched pathways include ETC and oxidative phosphorylation, proton membrane transport, and mitochondrial electron transport pathways (Fig. 4D). K-means and enrichment analyses between hCO samples supports previous findings while bringing further depth of understanding to how fabrication impacts specific hCO strengths.

Discussion

hCOs have revolutionized the way in which cardiac development and conditions can be modeled, providing scalable studies which mimic the cardiac environment in a manner superior to their 2D counterparts. Through a comprehensive investigation of bulk RNA-seq expression of carefully selected representative hCOs, we elucidated that alterations in fabrication results in heterogeneity between hCO models. Transcriptomic analyses provide vital insight into particular model strengths. We have identified an abundance of studies utilizing hCOs in a

multitude of applications, highlighting the numerous cardiac conditions, developmental pathways, and effects of cardioactive drugs to be modeled and better understood. This study presents a dedicated investigation using bulk RNA-seq, introducing an objective, data-driven relationship between hCO design and application.

Through PCA and clustering analysis, we found that hCOs profile similarly to one another in relation to CM-only and in vivo samples, replicating our previous findings in prior publications[34]. On the other hand, we found it compelling that as studies diverged from one another via differentiation protocol, means of tissue formation, and scale of time spent in culture, enrichment patterns also diverged. Upon investigating these divergences using GSEA, we found that a key indicator of how hCOs profiled in our analysis was the maturity of hCO components. Directed EB maturation drove hCO samples towards pathways of morphogenesis and embryonic development, showcasing a rapid hCO formation process. Meanwhile, using human primary cells increased hCO similarity to in vivo cardiac samples. We propose that this heterogeneity between means of hCO fabrication and subsequent transcriptomic phenotypes can be leveraged to tailor studies towards a suitable application. For instance, Drakhlis et al. describe a model intended to closely mimic fetal heart development, utilizing directed EB maturation[24]. Meanwhile, Ghosheh et al. develop an hCO model aiming to study electro-metabolic coupling of CMs, thus necessitating mature CMs[58]. This resulted in a fabrication with pre-differentiated cells rather than building an EB model, as a defined, mature population of cells was paramount. The complexities of the heart call for a multitude of models which have the potential to iteratively fill niches as advances in stem cell differentiation and tissue complexity capabilities are made.

Recent progress in hCO technology and understanding of cardiac developmental cues has improved biomimicry of the heart. Works from Giacomelli et al. have used hCOs to aid in understanding mechanisms of stromal populations that contribute to CVD[28]. Voges et al. provide insight into the vascular cell impact on CM maturation, building upon the HeartDyno hCO and emphasizing the importance of a comprehensive model[55]. While Schmidt et al. developed a multichambered fetal heart hCO model which closely mimics neonatal cardiogenesis, providing a platform to deepen our knowledge on how genetic mutations affect congenital heart disease[59]. Despite these breakthroughs, there remains a transcriptomic gap between hCOs and human tissue, highlighted in our GSVA analysis.

We acknowledge the technical limitations that our study imposes, from inclusion of a limited pool of representative studies, to the use of bulk RNA-seq samples. This study is not a comprehensive review of all hCO studies, but rather a snapshot of schools of thought within the field and how hCOs are to be approached. hCOs used in this study are at differing stages of development, which incurs inherent transcriptomic variability. However, we aim to highlight these differences as beneficial factors in the modeling of specific CVDs. Acquiring data publicly subsequently means that samples are not processed identically. To address this, we implemented batch correction between samples via normalization of counts before data analysis, but we do acknowledge potential differences between groups. Additionally, this study includes the use of solely bulk RNA-seq datasets, despite there being a wide range of -omics data publicly available. While bulk RNA-seq data is informative of the general transcriptomic profile of hCO models and cardiac tissue, it lacks the high resolution attainable with single cell RNA sequencing (scRNA-seq) and other forms of Next-Generation Sequencing (NGS) data. Using bulk RNA-seq data, we are only able to investigate tissue-level trends and are unable to delve into specific populations encapsulated within an hCO. This limits our ability to investigate some of the complexities and cell–cell crosstalk pathways within hCOs.

In summary, we selected four representative hCO studies, each focusing on distinct cardiac conditions and developmental aspects of the heart. Through clustering and enrichment analyses, we found that means of fabrication modulates hCO bulk RNA-seq profile, thus model development should be informed with application in mind. While the maturity of hCOs still lags behind that of human myocardium, ongoing research aims to enhance biomimicry by improving vascular networks, integrating immune cells, and refining hiPSC differentiation protocols. Our study suggests that a key component to maximize hCO effectiveness as a model for CVD is to utilize the proper fabrication method for its intended use.

Materials and methods

Sourcing publicly available FASTQ data

We compiled bulk RNA-seq datasets from four unique hCOs to provide a wholistic overview of the current hCO field[27,29,30,33]. These four studies were selected as they embody a range of fabrication methods, from 3D EB-based cardiac differentiation to engineered microtissue assembly. Publicly available bulk RNA FASTQ files were acquired from both Gene Expression Omnibus (GEO) as well as the European Nucleotide Archive (ENA) databases. 2D hiPSC-CM (GSE91383), along with 3D hiPSC-CM samples (GSE181397) were obtained to serve as mono-cellular benchmarks. Following this, four hCO models possessing publicly available bulk RNA sequencing data were identified via literature review (GSE209997, GSE93841, GSE113871, GSE153185). As the aim of many of these hCOs is to provide a platform to better model various aspects and pathologies of the heart, human fetal (GSE62913) and adult cardiac tissue (GSE62913, GSE93841). Total FASTQ files from each study were downloaded and catalogued in Microsoft Excel for recordkeeping. All schematics of representative studies and experimental workflow were drawn with BioRender.

Genome alignment and generation of gene counts files

Desired sample FASTQ files were loaded into the online Galaxy tool (v23.2.1). Before mapping to a human genome, the raw files were tested for quality and trimmed using the Trimmomatic tool within Galaxy (v0.38). To generate counts data, the RNA STAR function (v2.7.10b) was first used to map each sample to Human Genome 38 (hg38), which generated a mapped .bam file. A function called featureCounts (v2.0.3) then utilized the .bam

file and translate it into a tabular raw gene counts file, which was downloaded and merged into an Excel (version 2310) file containing gene counts for all samples.

Principal component analysis

Principal Component Analysis (PCA) was performed using the Bioconductor (v3.16) package within the RStudio (v2023.03.0) workspace. Desired sample gene matrices were loaded into the workspace. Geneids were mapped to gene symbols, for better understanding and ease of use. For PCA analysis, the Bioconductor package "DESeq2" (v1.38.3) was used to generate differentially expressed gene matrices for all samples. Any gene counts containing zero or one read across all samples were removed, and an rlog transformation was done to normalize data. The differentially expressed gene matrix was scaled by Z-score. Following this, the scaled matrix was subjected to a principal component computation. A PC plot utilized PC1 and PC2, the top two axes driving variation between samples, and plotted samples in a scatterplot format, visualized with the "ggplot2" package (v3.4.2). Additionally, a heatmap representing sample distances relative to each other based upon this principal component computation was generated.

Gene set enrichment analysis (GSEA)

Directly using the PC1 and PC2 readouts from PC computations, a gene set enrichment analysis (GSEA) was executed[41]. The top 100 variable genes influencing sample differences are used in this analysis. From the PC computation, the first column of data (PC1 loadings) and the second column of data (PC2 loadings) for each of these 500 variable genes are isolated in RStudio and saved as a .rnk file. This .rnk file is then loaded into GSEA software (v 4.3.0) from the BROAD institute, and a GSEA Preranked analysis is executed. The scope of our study was to uncover biological processes and pathways which could contribute to specific diseases; therefore, we utilized the GO term biological processes pathway dataset (c5.go.v2023.Hs.symbols.gmt) provided by the BROAD institute run our analysis through. Pathways containing less than 15 gene hits and more than 500 gene hits were excluded from the study. Pathways that were significant at FDR < 0.250 were included as viable pathways for this study. GraphPad (v.3.2) was then utilized to visualize GSEA results using normalized enrichment scores (NES) of each individual pathway.

K-means clustering analysis

K-means clustering analysis was conducted through RStudio, making use of the previously described differentially expressed gene matrices via DESeq2 and rlog transformations. To identify which genes to use for K means analysis, the normalized counts are trimmed to counts with a variance and mean above 50, meaning only high gene counts that are of the most variance are used for this analysis. The top 100 genes influencing variability between samples are then used. Four clusters were determined to be the ideal number by which to sort the top 100 genes, and the data was visualized in a heatmap. Metascape was also used as a tool to generate gene-related pathways for each cluster. Gene lists for each cluster consisting of only gene symbols were loaded into Metascape, which provided information about pathways and the relativity of genes within said cluster.

Gene set variation analysis (GSVA)

Cardiac cell gene sets were constructed from the publicly available Heart Cell Atlas dataset[54]. Using their nomenclature, the 50 genes with the highest expression in each subcategory of cardiac cell were used to build these custom gene sets for Gene Set Variation Analysis (GSVA). The following cell groups were used to subcategorize cell gene sets: (1) ventricular cardiomyocytes, (2) atrial cardiomyocytes, (3) ventricular fibroblasts, (4) endothelial cells, (5) immune cells. These subcategories are derived from supplementary tables 6 (cardiomyocytes), 11 (fibroblasts), 14 (immune cells).

Data availability

Raw and normalized counts files are available in the NCBI GEO public repository with accession no. GSE24573816. The data acquired and analyzed within this manuscript can be found with the gene expression omnibus (GEO) under accession numbers GSE91383 (2D CMs), GSE181397 (3D CMs), GSE153185 (EB hCO), GSE209997 (Extended Culture hCO), GSE93841 (HeartDyno hCO), GSE113871 (Primary Stroma hCO), GSE62913 (Fetal and Adult Cardiac Tissue).

Received: 8 March 2024; Accepted: 7 May 2024
Published online: 30 August 2024

References

1. Vos, T. *et al.* Global burden of 369 diseases and injuries in 204 countries and territories, 1990–2019: A systematic analysis for the Global Burden of Disease Study 2019. *Lancet* **396**(10258), 1204–1222. https://doi.org/10.1016/S0140-6736(20)30925-9 (2020).
2. Forouzanfar, M. H. *et al.* Assessing the global burden of ischemic heart disease: part 2: Analytic methods and estimates of the global epidemiology of ischemic heart disease in 2010. *Glob. Heart* **7**(4), 331. https://doi.org/10.1016/j.gheart.2012.10.003 (2012).
3. Jensen, R. V., Hjortbak, M. V. & Bøtker, H. E. Ischemic heart disease: An update. *Semin. Nucl. Med.* **50**(3), 195–207. https://doi.org/10.1053/j.semnuclmed.2020.02.007 (2020).
4. Giudice, V., Vecchione, C. & Selleri, C. Cardiotoxicity of novel targeted hematological therapies. *Life* **10**(12), 344. https://doi.org/10.3390/life10120344 (2020).
5. Hofer, M. & Lutolf, M. P. Engineering organoids. *Nat. Rev. Mater.* **6**(5), 402–420. https://doi.org/10.1038/s41578-021-00279-y (2021).
6. Drakhlis, L. & Zweigerdt, R. Heart in a dish – choosing the right *in vitro* model. *Dis. Model. Mech.* **16**(5), dmm049961. https://doi.org/10.1242/dmm.049961 (2023).

7. Vunjak Novakovic, G., Eschenhagen, T. & Mummery, C. Myocardial tissue engineering: In vitro models Cold Spring Harb. *Perspect. Med.* **4**(3), 014076–014076. https://doi.org/10.1101/cshperspect.a014076 (2014).
8. Rossi, G., Manfrin, A. & Lutolf, M. P. Progress and potential in organoid research. *Nat. Rev. Genet.* **19**(11), 671–687. https://doi.org/10.1038/s41576-018-0051-9 (2018).
9. Correia, C. *et al.* 3D aggregate culture improves metabolic maturation of human pluripotent stem cell derived cardiomyocytes. *Biotechnol. Bioeng.* **115**(3), 630–644. https://doi.org/10.1002/bit.26504 (2018).
10. Cesarovic, N., Lipiski, M., Falk, V. & Emmert, M. Y. Animals in cardiovascular research. *Eur. Heart J.* **41**(2), 200–203. https://doi.org/10.1093/eurheartj/ehz933 (2020).
11. Lian, X. *et al.* Robust cardiomyocyte differentiation from human pluripotent stem cells via temporal modulation of canonical Wnt signaling. *Proc. Natl. Acad. Sci.* **109**, 27. https://doi.org/10.1073/pnas.1200250109 (2012).
12. Lian, X., Zhang, J., Zhu, K., Kamp, T. J. & Palecek, S. P. Insulin inhibits cardiac mesoderm, not mesendoderm, formation during cardiac differentiation of human pluripotent stem cells and modulation of canonical wnt signaling can rescue this inhibition. *Stem Cells* **31**(3), 447–457. https://doi.org/10.1002/stem.1289 (2013).
13. Zhang, J. Z. *et al.* A human iPSC double-reporter system enables purification of cardiac lineage subpopulations with distinct function and drug response profiles. *Cell Stem Cell* **24**(5), 802–811. https://doi.org/10.1016/j.stem.2019.02.015 (2019).
14. Takahashi, K. *et al.* Induction of pluripotent stem cells from adult human fibroblasts by defined factors. *Cell* **131**(5), 861–872. https://doi.org/10.1016/j.cell.2007.11.019 (2007).
15. Sharma, A., Wu, J. C. & Wu, S. M. Induced pluripotent stem cell-derived cardiomyocytes for cardiovascular disease modeling and drug screening. *Stem Cell Res. Ther.* **4**(6), 150. https://doi.org/10.1186/scrt380 (2013).
16. Dubois, N. C. *et al.* SIRPA is a specific cell-surface marker for isolating cardiomyocytes derived from human pluripotent stem cells. *Nat. Biotechnol.* **29**(11), 1011–1018. https://doi.org/10.1038/nbt.2005 (2011).
17. Musunuru, K. *et al.* Induced pluripotent stem cells for cardiovascular disease modeling and precision medicine: A scientific statement from the American heart association. *Circ Genomic Precis Med* **11**, 1. https://doi.org/10.1161/HCG.0000000000000043 (2018).
18. Sacchetto, C., Vitiello, L., De Windt, L. J., Rampazzo, A. & Calore, M. Modeling cardiovascular diseases with hiPSC-derived cardiomyocytes in 2D and 3D cultures. *Int. J. Mol. Sci.* **21**(9), 3404. https://doi.org/10.3390/ijms21093404 (2020).
19. Branco, M. A. *et al.* Transcriptomic analysis of 3D cardiac differentiation of human induced pluripotent stem cells reveals faster cardiomyocyte maturation compared to 2D culture. *Sci. Rep.* **9**(1), 9229. https://doi.org/10.1038/s41598-019-45047-9 (2019).
20. Fontoura, J. C. *et al.* Comparison of 2D and 3D cell culture models for cell growth, gene expression and drug resistance. *Mater. Sci. Eng. C* **107**, 110264. https://doi.org/10.1016/j.msec.2019.110264 (2020).
21. Scalise, M. *et al.* From spheroids to organoids: The next generation of model systems of human cardiac regeneration in a dish. *Int. J. Mol. Sci.* **22**(24), 13180. https://doi.org/10.3390/ijms222413180 (2021).
22. Scalise, M. *et al.* Adult multipotent cardiac progenitor-derived spheroids: A reproducible model of in vitro cardiomyocyte commitment and specification. *Cells* **12**(13), 1793. https://doi.org/10.3390/cells12131793 (2023).
23. Hofbauer, P. *et al.* Cardioids reveal self-organizing principles of human cardiogenesis. *Cell* **184**(12), 3299-3317.e22. https://doi.org/10.1016/j.cell.2021.04.034 (2021).
24. Drakhlis, L. *et al.* Human heart-forming organoids recapitulate early heart and foregut development. *Nat. Biotechnol.* **39**(6), 737–746. https://doi.org/10.1038/s41587-021-00815-9 (2021).
25. Branco, M. A., Dias, T. P., Cabral, J. M. S., Pinto-do-Ó, P. & Diogo, M. M. Human multilineage pro-epicardium/foregut organoids support the development of an epicardium/myocardium organoid. *Nat. Commun.* **13**(1), 6981. https://doi.org/10.1038/s41467-022-34730-7 (2022).
26. Frum, T. & Spence, J. R. hPSC-derived organoids: models of human development and disease. *J. Mol. Med.* **99**(4), 463–473. https://doi.org/10.1007/s00109-020-01969-w (2021).
27. Lewis-Israeli, Y. R. *et al.* Self-assembling human heart organoids for the modeling of cardiac development and congenital heart disease. *Nat. Commun.* **12**(1), 5142. https://doi.org/10.1038/s41467-021-25329-5 (2021).
28. Giacomelli, E. *et al.* Human-iPSC-derived cardiac stromal cells enhance maturation in 3D cardiac microtissues and reveal non-cardiomyocyte contributions to heart disease. *Cell Stem Cell* **26**(6), 862-879.e11. https://doi.org/10.1016/j.stem.2020.05.004 (2020).
29. Ergir, E. *et al.* Generation and maturation of human iPSC-derived 3D organotypic cardiac microtissues in long-term culture. *Sci. Rep.* **12**(1), 17409. https://doi.org/10.1038/s41598-022-22225-w (2022).
30. Mills, R. J. *et al.* Functional screening in human cardiac organoids reveals a metabolic mechanism for cardiomyocyte cell cycle arrest. *Proc. Natl. Acad. Sci.* **114**, 40. https://doi.org/10.1073/pnas.1707316114 (2017).
31. Richards, D. J. *et al.* Inspiration from heart development: Biomimetic development of functional human cardiac organoids. *Biomaterials* **142**, 112–123. https://doi.org/10.1016/j.biomaterials.2017.07.021 (2017).
32. Arhontoulis, D. C. *et al.* Human cardiac organoids to model COVID-19 cytokine storm induced cardiac injuries. *J. Tissue Eng. Regen. Med.* **16**(9), 799–811. https://doi.org/10.1002/term.3327 (2022).
33. Richards, D. J. *et al.* Human cardiac organoids for the modelling of myocardial infarction and drug cardiotoxicity. *Nat. Biomed. Eng.* **4**(4), 446–462. https://doi.org/10.1038/s41551-020-0539-4 (2020).
34. Kerr, C. M., Richards, D., Menick, D. R., Deleon-Pennell, K. Y. & Mei, Y. Multicellular human cardiac organoids transcriptomically model distinct tissue-level features of adult myocardium. *Int. J. Mol. Sci.* **22**(16), 8482. https://doi.org/10.3390/ijms22168482 (2021).
35. Necela, B. M. *et al.* The antineoplastic drug, trastuzumab, dysregulates metabolism in iPSC-derived cardiomyocytes. *Clin. Transl. Med.* **6**, 1. https://doi.org/10.1186/s40169-016-0133-2 (2017).
36. Kuppusamy, K. T. *et al.* Let-7 family of microRNA is required for maturation and adult-like metabolism in stem cell-derived cardiomyocytes. *Proc. Natl. Acad. Sci.* **112**, 21. https://doi.org/10.1073/pnas.1424042112 (2015).
37. . J. Matkovich and G. W. Dorn, "Deep sequencing of cardiac MicroRNA-mRNA interactomes in clinical and experimental cardiomyopathy," in *Cardiomyocytes*, vol. 1299, G. R. Skuse and M. C. Ferran, Eds., in Methods in Molecular Biology, vol. 1299. , New York, NY: Springer New York, 2015, pp. 27–49. doi: https://doi.org/10.1007/978-1-4939-2572-8_3
38. Huber, W. *et al.* Orchestrating high-throughput genomic analysis with Bioconductor. *Nat. Methods* **12**(2), 115–121. https://doi.org/10.1038/nmeth.3252 (2015).
39. Bedada, F. B., Wheelwright, M. & Metzger, J. M. 2016 Maturation status of sarcomere structure and function in human iPSC-derived cardiac myocytes. *Biochim. Biophys. Acta BBA – Mol. Cell Res.* **7**, 1829–1838. https://doi.org/10.1016/j.bbamcr.2015.11.005 (1863).
40. Yang, X., Pabon, L. & Murry, C. E. Engineering adolescence: maturation of human pluripotent stem cell-derived cardiomyocytes. *Circ. Res.* **114**(3), 511–523. https://doi.org/10.1161/CIRCRESAHA.114.300558 (2014).
41. Subramanian, A. *et al.* Gene set enrichment analysis: A knowledge-based approach for interpreting genome-wide expression profiles. *Proc. Natl. Acad. Sci.* **102**(43), 15545–15550. https://doi.org/10.1073/pnas.0506580102 (2005).
42. Mohr, J. C. *et al.* The microwell control of embryoid body size in order to regulate cardiac differentiation of human embryonic stem cells. *Biomaterials* **31**(7), 1885–1893. https://doi.org/10.1016/j.biomaterials.2009.11.033 (2010).
43. Sinaga, K. P. & Yang, M.-S. Unsupervised K-means clustering algorithm. *IEEE Access* **8**, 80716–80727. https://doi.org/10.1109/ACCESS.2020.2988796 (2020).
44. Komori, T. Regulation of bone development and extracellular matrix protein genes by RUNX2. *Cell Tissue Res.* **339**(1), 189–195. https://doi.org/10.1007/s00441-009-0832-8 (2010).

45. Chimenti, I., Gaetani, R. & Pagano, F. Editorial: The cardiac stroma in homeostasis and disease. *Front. Cardiovasc. Med.* **10**, 1248750. https://doi.org/10.3389/fcvm.2023.1248750 (2023).
46. Zhou, Y. *et al.* Metascape provides a biologist-oriented resource for the analysis of systems-level datasets. *Nat. Commun.* **10**(1), 1523. https://doi.org/10.1038/s41467-019-09234-6 (2019).
47. Cho, S., Discher, D. E., Leong, K. W., Vunjak-Novakovic, G. & Wu, J. C. Challenges and opportunities for the next generation of cardiovascular tissue engineering. *Nat. Methods* **19**(9), 1064–1071. https://doi.org/10.1038/s41592-022-01591-3 (2022).
48. Smits, P., Smeitink, J. & Van Den Heuvel, L. Mitochondrial translation and beyond: processes implicated in combined oxidative phosphorylation deficiencies. *J. Biomed. Biotechnol.* **2010**, 1–24. https://doi.org/10.1155/2010/737385 (2010).
49. Gubina, N. E., Merekina, O. S. & Ushakova, T. E. Mitochondrial DNA transcription in mouse liver, skeletal muscle, and brain following lethal X-ray irradiation. *Biochem. Mosc.* **75**(6), 777–783. https://doi.org/10.1134/S0006297910060131 (2010).
50. Kolwicz, S. C., Purohit, S. & Tian, R. Cardiac metabolism and its interactions with contraction, growth, and survival of cardiomyocytes. *Circ. Res.* **113**(5), 603–616. https://doi.org/10.1161/CIRCRESAHA.113.302095 (2013).
51. Flaim, C. J., Teng, D., Chien, S. & Bhatia, S. N. Combinatorial signaling microenvironments for studying stem cell fate. *Stem Cells Dev.* **17**(1), 29–40. https://doi.org/10.1089/scd.2007.0085 (2008).
52. Posch, M. G. *et al.* Cardiac alpha-myosin (MYH6) is the predominant sarcomeric disease gene for familial atrial septal defects. *PLoS ONE* **6**(12), e28872. https://doi.org/10.1371/journal.pone.0028872 (2011).
53. Hänzelmann, S., Castelo, R. & Guinney, J. GSVA: gene set variation analysis for microarray and RNA-Seq data. *BMC Bioinformatics* **14**(1), 7. https://doi.org/10.1186/1471-2105-14-7 (2013).
54. Litviňuková, M. *et al.* Cells of the adult human heart. *Nature* **588**(7838), 466–472. https://doi.org/10.1038/s41586-020-2797-4 (2020).
55. Voges, H. K. *et al.* Vascular cells improve functionality of human cardiac organoids. *Cell Rep.* https://doi.org/10.1016/j.celrep.2023.112322 (2023).
56. Liang, P.-Y., Chang, Y., Jin, G., Lian, X. & Bao, X. Wnt signaling directs human pluripotent stem cells into vascularized cardiac organoids with chamber-like structures. *Front. Bioeng. Biotechnol.* **10**, 1059243. https://doi.org/10.3389/fbioe.2022.1059243 (2022).
57. Lidington, E., Moyes, D., McCormack, A. & Rose, M. A comparison of primary endothelial cells and endothelial cell lines for studies of immune interactions. *Transpl. Immunol.* **7**(4), 239–246. https://doi.org/10.1016/S0966-3274(99)80008-2 (1999).
58. Ghosheh, M. *et al.* Electro-metabolic coupling in multi-chambered vascularized human cardiac organoids. *Nat. Biomed. Eng.* https://doi.org/10.1038/s41551-023-01071-9 (2023).
59. Schmidt, C. *et al.* Multi-chamber cardioids unravel human heart development and cardiac defects. *Cell* **186**(25), 5587-5605.e27. https://doi.org/10.1016/j.cell.2023.10.030 (2023).

Author contributions

N.A.H., C.M.K, and Y.M. designed and conceived the study. N.A.H. and C.M.K performed the experiments and data analysis. N.A.H. performed RNA-seq data compilation and genome alignment. N.A.H. performed PCA, K-means clustering, GSEA, and GSVA, with assistance from C.M.K. Data visualization was performed by N.A.H. D.C.A. provided insight into GO Term analysis interpretation. N.A.H. led the original manuscript preparation with C.M.K and D.C.A. J.M.R., Y.M., C.M.K., and D.C.A. led the review and editing of the manuscript.

Funding

This research is funded by the National Institutes of Health (1F31HL154665, 1F30HL160055, 8P20 GM103444, 1R01HL133308, 1U01HL169361, 1R01HL168255, 1R21HL167211, UL1TR001450). This work was also supported by American Heart Association Grant # 23IPA1054426/Ying Mei/2023 and the National Science Foundation (NSF) Award #OIA-2242812.

Competing interests

The authors declare no competing interests.

Additional information

Supplementary Information The online version contains supplementary material available at https://doi.org/10.1038/s41598-024-61554-w.

Correspondence and requests for materials should be addressed to Y.M.